HHS Public Access

Author manuscript

Adv Funct Mater. Author manuscript; available in PMC 2017 March 08.

Published in final edited form as:

Adv Funct Mater. 2016 March 8; 26(10): 1628–1635. doi:10.1002/adfm.201505231.

Nanoparticle-Based Antivirulence Vaccine for the Management of Methicillin-Resistant *Staphylococcus aureus* Skin Infection

Fei Wang,
Department of NanoEngineering and Moores Cancer Center, University of California, San Diego, La Jolla, CA 92093, U.S.A. Department of Pharmaceutics, School of Pharmacy, Fudan University, and Key Laboratory of Smart Drug Delivery (Fudan University), Ministry of Education, Shanghai 201203, P.R. China

Dr. Ronnie H. Fang,
Department of NanoEngineering and Moores Cancer Center, University of California, San Diego, La Jolla, CA 92093, U.S.A

Brian T. Luk,
Department of NanoEngineering and Moores Cancer Center, University of California, San Diego, La Jolla, CA 92093, U.S.A

Dr. Che-Ming J. Hu,
Department of NanoEngineering and Moores Cancer Center, University of California, San Diego, La Jolla, CA 92093, U.S.A. Institute of Biomedical Sciences, Academia Sinica, Taipei, Taiwan

Dr. Soracha Thamphiwatana,
Department of NanoEngineering and Moores Cancer Center, University of California, San Diego, La Jolla, CA 92093, U.S.A

Diana Dehaini,
Department of NanoEngineering and Moores Cancer Center, University of California, San Diego, La Jolla, CA 92093, U.S.A

Pavimol Angsantikul,
Department of NanoEngineering and Moores Cancer Center, University of California, San Diego, La Jolla, CA 92093, U.S.A

Ashley V. Kroll,
Department of NanoEngineering and Moores Cancer Center, University of California, San Diego, La Jolla, CA 92093, U.S.A

Dr. Zhiqing Pang,
Department of NanoEngineering and Moores Cancer Center, University of California, San Diego, La Jolla, CA 92093, U.S.A. Department of Pharmaceutics, School of Pharmacy, Fudan University, and Key Laboratory of Smart Drug Delivery (Fudan University), Ministry of Education, Shanghai 201203, P.R. China

Dr. Weiwei Gao,

Correspondence to: Liangfang Zhang, zhang@ucsd.edu.

Department of NanoEngineering and Moores Cancer Center, University of California, San Diego, La Jolla, CA 92093, U.S.A

Prof. Weiyue Lu, and
Department of Pharmaceutics, School of Pharmacy, Fudan University, and Key Laboratory of Smart Drug Delivery (Fudan University), Ministry of Education, Shanghai 201203, P.R. China

Prof. Liangfang Zhang
Department of NanoEngineering and Moores Cancer Center, University of California, San Diego, La Jolla, CA 92093, U.S.A

Liangfang Zhang: zhang@ucsd.edu

Abstract

With the rising threat of antibiotic-resistant bacteria, vaccination is becoming an increasingly important strategy to prevent and manage bacterial infections. Made from deactivated bacterial toxins, toxoid vaccines are widely used in the clinic as they help to combat the virulence mechanisms employed by different pathogens. Herein, the efficacy of a biomimetic nanoparticle-based anti-virulence vaccine is examined in a mouse model of methicillin-resistant *Staphylococcus aureus* (MRSA) skin infection. Vaccination with nanoparticle-detained staphylococcal α-hemolysin (Hla) effectively triggers the formation of germinal centers and induces high anti-Hla titers. Compared to mice vaccinated with control samples, those vaccinated with the nanoparticle toxoid show superior protective immunity against MRSA skin infection. The vaccination not only inhibits lesion formation at the site of bacterial challenge, but also reduces the invasiveness of MRSA, preventing dissemination into other organs. Overall, this biomimetic nanoparticle-based toxin detainment strategy is a promising method for the design of potent anti-virulence vaccines for managing bacterial infections.

Graphical Abstract

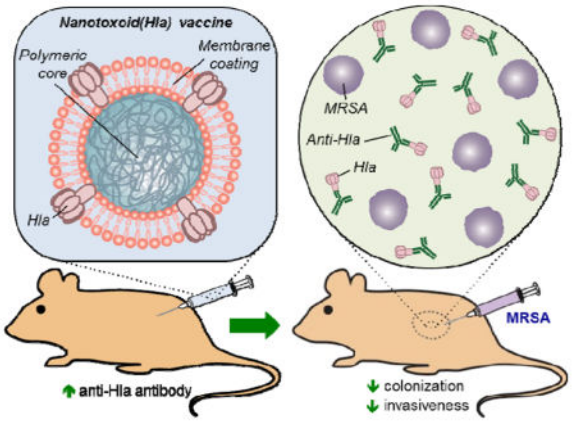

A nanoparticle-based strategy is employed to effectively neutralize and retain bacterial toxins, enabling safe delivery *in vivo* for anti-virulence vaccination. The ability of this approach to elicit potent antitoxin immune responses and protect against live bacterial infection is studied using a murine model of methicillin-resistant *Staphylococcus aureus* (MRSA) skin infection with α-hemolysin as the toxin of interest.

Keywords

biomimetic nanoparticle; toxoid; anti-virulence vaccination; α-hemolysin; MRSA infection

1. Introduction

The continued rise of antibiotic-resistant bacteria has become a significant burden on global health and is responsible for an increased rate of life-threatening infections observed in the clinic.[1] The issue continues to rise to the forefront as the development of new antibiotics has slowed to a near halt,[2] prompting physicians and scientists to explore alternative strategies to control bacterial infections.[3] Among the different approaches, anti-virulence vaccination is a compelling strategy as it promotes host immunity by training the body to detect and disarm specific mechanisms employed by pathogens during host invasion.[4] This approach has been shown to inhibit the ability of pathogens to colonize within a host and is less susceptible to the development of resistance as it does not exert direct selective pressure on individual bacterium.[5] Anti-virulence vaccination is most commonly accomplished through the use of toxoids, or inactivated forms of live bacterial toxins, which include the commonly used tetanus toxoid[6] and diphtheria toxoid.[7] Conventionally, these toxoids are prepared by denaturation via either chemical or heat treatment in order to eliminate the dangerous effects of the original toxin.[8] However, such inactivation methods are often disruptive and can lead to altered antigen presentation as well as compromised immunogenicity.[9] To overcome the tradeoff between safety and efficacy, emerging techniques are being developed to produce vaccine candidates that faithfully present antigenic epitopes for immune processing.[10]

Methicillin-resistant *Staphylococcus aureus* (MRSA) is an antibiotic-resistant pathogen that represents a significant threat to public health, especially in hospital environments where many patients have weakened immune systems that are incapable of naturally fending off infection.[11] It can cause severe skin lesions and can ultimately be life-threatening upon systemic invasion.[12] The pace of resistance exhibited by MRSA has severely limited treatment options, with many strains of the bacteria being unresponsive to all of the most commonly used antibiotics.[13, 14] This has led researchers to explore other forms of treatment, including the aforementioned anti-virulence therapy. Known to secrete many different types of exotoxins, MRSA represents a good target for such therapies. One of its major virulence factors is α-hemolysin (Hla),[15] a toxin that forms heptameric pores on cell surfaces, which contributes greatly to the pathogenesis of MRSA during the process of infection.[16] In fact, it has been shown that the virulence of the pathogen correlates strongly with the level of Hla production.[17, 18] Further, immunization with a mutant form of Hla has been shown to confer protection against *Staphylococcus aureus* (*S. aureus)* pneumonia in mice.[19] Passive immunization with anti-Hla antibodies also protected against skin lesions caused by subsequent *S. aureus* infection, further attesting to the utility of such a strategy for combating the pathogen.

The application of novel nanomaterials towards vaccine design has the potential to bring about significant improvements via efficient and finely controlled immune

manipulation.[20–25] We have previously demonstrated a nanoparticle-mediated toxin detainment strategy for the preparation of a safe and potent toxoid formulation. Biomimetic nanoparticles are fabricated with a cell membrane-derived coating that presents a natural substrate for pore-forming toxins,[26, 27] leading to their stable entrapment onto the nanoparticles and enabling safe delivery *in vivo* for immune processing.[28] Owing to the non-disruptive approach of this detainment strategy, the platform was demonstrated to be superior to a traditionally formed toxoid by generating higher anti-Hla titers with increased avidity. Further, vaccination with the detained toxin conferred a significant survival benefit in a murine model of lethal toxin challenge. In the present work, we investigated the protective capabilities of nanoparticle-detained staphylococcal Hla, denoted nanotoxoid(Hla), against live bacterial challenge using a mouse model of MRSA skin infection (Figure 1). The immune potentiating effect of the nanoparticle formulation was studied more in-depth by looking at the formation of germinal centers in the draining lymph nodes of vaccinated mice, which was then correlated to anti-Hla titer production. The ability of the nanotoxoid(Hla) vaccine to protect against MRSA infection and lessen bacterial colonization was evaluated in a mouse model of skin lesion formation. Beyond local infection, the effect of the nanoparticle vaccination on bacterial invasiveness was further studied by enumerating the bacterial load in major organs.

2. Results and Discussion

2.1. Nanotoxoid(Hla) Synthesis and Characterization

Nanoparticles coated with red blood cell (RBC) membrane were prepared using a previously described protocol.[29] Briefly, mouse RBCs were subjected to hypotonic treatment to obtain purified RBC membrane ghosts, which were then fused onto the surface of preformed nanoparticle cores made using poly(lactic-*co*-glycolic acid) (PLGA) through a sonication method. As the RBC membrane coating serves as a natural substrate for the pore-forming Hla, nanotoxoid(Hla) complexes were formed by incubating free Hla with unloaded nanoparticles, herein denoted nanotoxoid(−). Free Hla was subsequently removed from the nanotoxoid(Hla) complexes by size exclusion chromatography to obtain a purified formulation. Physicochemical characterization showed that the resulting nanotoxoid(Hla) was about 115 nm in diameter and had a surface zeta potential of −32 mV (Figure 2a,b), both of which were similar to those of the unloaded nanotoxoid(−), suggesting that toxin insertion did not have a major impact on overall nanoparticle properties. This was further confirmed via transmission electron microscopy (TEM) of negatively stained nanotoxoid(Hla), which revealed that the characteristic core-shell structure of the RBC membrane-coated nanoparticle was preserved even after toxin loading, consistent with what has been previously observed[26, 28] (Figure 2c).

To confirm successful detainment of Hla by the RBC membrane-coated nanoparticles, different immunoassays were performed. On TEM image, Hla-specific antibody labeling of nanotoxoid(Hla) followed by secondary labeling using an immunogold conjugate showed significant colocalization of the electron-dense gold signal with regions of intermediate density occupied by the nanoparticles, indicating a significant presence of Hla-specific epitopes on the nanotoxoid(Hla) (Figure 2d). Conversely, nanotoxoid(−) sample subjected to

the exact same staining procedure was absent of any gold signal, confirming that the positive signal seen in the nanotoxoid(Hla) was not due to non-specific antibody staining. Note that in the absence of negative staining, the morphological appearance of the nanotoxoid differs from what is observed in Figure 3c. The uranyl acetate stain can act as a fixative, serving to stabilize the nanoparticles and to enhance the core-shell structure of the nanoparticles. Dot blot analysis was used to further confirm the presence of Hla on nanotoxoid(Hla) samples (Figure 2e). Using anti-Hla as the primary immunostain, nanotoxoid(Hla) gave a positive signal whereas nanotoxoid(−) did not give any discernable signal. As a positive control, free Hla at the initial input concentration used to prepare nanotoxoid(Hla) was tested in parallel, and image analysis of the blot intensities revealed that approximately 95% of the Hla was retained on the nanoparticles after purification, suggesting high affinity of the toxin for the membrane-coated nanoparticles. It has been shown previously that the strong sequestration of toxin by the nanoparticle detainment strategy resulted in little release over time, which effectively neutralized the activity of the toxin and enables safe delivery both *in vitro* and *in vivo*.[28]

2.2. Humoral Immune Response Characterization

Next, the ability of the nanotoxoid(Hla) formulation to promote anti-Hla immune responses was studied. Of particular interest was the formation of germinal centers (GCs), which is a critical step in the potentiation of the humoral immune response against foreign antigens.[30, 31] It is in these regions that B cells mature, and it has been shown that improved retention of antigens via nanoparticle-mediated delivery can better facilitate GC formation.[32] We therefore sought to evaluate lymphatic B cell activation in mice immunized with the nanotoxoid(Hla) formulation. Immunostaining was employed to detect the presence of GCs in the draining lymph nodes (dLNs) of mice immunized subcutaneously with the nanoformulation. PBS and unloaded nanotoxoid(−) were administered as controls. Histological analysis of the dLNs from mice immunized with nanotoxoid(Hla) revealed GL-7$^+$ regions characteristic of GC nucleation (Figure 3a). In contrast, there was no visual evidence of GC formation in the PBS or nanotoxoid(−) immunization groups, confirming the non-immunogenicity of the naturally derived nanoparticle vector itself.[33] Flow cytometry results (Figure 3b) showed that 45.6% of B220$^+$IgD^{low} B cells in the dLNs of the nanotoxoid(Hla) group exhibited a GL-7$^+$ germinal center phenotype. In contrast, only 15.7% and 13.6% of cells in mice administered with PBS and nanotoxoid(−), respectively, exhibited the same phenotype.

The ability of nanotoxoid(Hla) to elicit a humoral immune response against Hla was further investigated. Mice were subcutaneously injected with nanotoxoid(Hla), nanotoxoid(−) or PBS on day 0 and were subsequently administered a booster on day 14. The serum of the mice in each group was sampled on days 0, 14 and 35 to assess Hla-specific IgG titers (Figure 3c–e). Nanotoxoid(Hla) vaccination elicited significant anti-Hla titers on day 14, and there was a further increase when assayed on day 35. In contrast, the nanotoxoid(−) and PBS vaccinations resulted in no detectable anti-Hla titers over the course of the study. The nanotoxoid(Hla)-induced antibody responses have previously been shown to be durable, with little to no drop in titers over the course of a five-month period.[28] Taken together, the data demonstrates that the nanotoxoid(Hla) formulation can effectively elicit potent anti-Hla

immune responses, despite complete deactivation of the toxin.[26] This is notable finding given that the formulation is absent of immunological adjuvants, which are commonly required for conventional toxoid formulations and help to boost germinal center antibody activity.[34]

2.3. Efficacy in a Mouse Model of MRSA Skin Infection

To evaluate the protective capability of the nanotoxoid(Hla) vaccine against MRSA infection, we employed a mouse skin infection model. MRSA represents one of the most common causes of skin infections, both in the community and in hospitals.[12] Because the pathogen is hard to treat with common antibiotics, the infection can quickly progress and lead to serious complications, from physical disfigurement to permanent organ damage, and in many cases even death. For this experiment, mice were immunized with nanotoxoid(Hla) on day 0 and given a booster dose on day 14. Mice injected with nanotoxoid(−) or PBS were used as control groups. On day 35, the mice were subcutaneously challenged with live MRSA bacteria, and the efficacy in the different experimental groups was assessed over time by monitoring the dermonecrotic area resulting from bacterial burden. The progression of skin lesion development in mice immunized with nanotoxoid(Hla) was significantly attenuated compared with mice in the nanotoxoid(−) and PBS groups, which both experienced rapid lesion formation (Figure 4a,b). On day 6 post-infection, there was an approximately 5-fold reduction in dermonecrotic area on mice treated with the nanotoxoid(Hla) formulation compared to the control groups.

At the conclusion of the observation period, the bacterial burden was quantified in the infected skin region of each mouse (Figure 4c). For the nanotoxoid(−) and PBS groups, the bacterial burden of the infected skin tissue was 1.7×10^7 and 2.2×10^7 CFU, respectively. Mice immunized with nanotoxoid(Hla) showed an average burden of 1.5×10^6 CFU, representing an 11.3- and 14.7-fold reduction compared with the nanotoxoid(−) and PBS groups, respectively. It has previously been shown that nanotoxoid(Hla) is capable of significantly inhibiting Hla-mediated skin damage in the subcutaneous space, suggesting that the titers generated by the formulation are sufficiently high to enable extravascular neutralizing activity.[28] This prevents the necrotic effect of high Hla concentrations,[35] thus preserving integrity of the local tissue. In the present study, the nanoparticle vaccine formulation was likewise able to reduce skin lesion formation, demonstrating its ability to facilitate neutralization of Hla produced by the bacteria *in situ* upon subcutaneous challenge. Given the importance of Hla in MRSA pathogenesis, neutralization of the toxin also resulted in decreased bacterial burden, likely due to increased clearance by immune cells protected from the cytotoxic activity of Hla.[36] Despite the significant reduction in both lesion formation and bacterial load at the site of infection, the inability of the nanotoxoid(Hla) to completely mitigate disease suggests a sizable role played by other virulence factors, which can serve as targets for future nanotoxoid vaccine formulations.

2.4. Prevention of Disseminative MRSA Infection

MRSA infections can quickly progress and enter systemic circulation, leading to a markedly worse prognosis in the clinic.[11] Patients with invasive MRSA can precipitously develop life-threatening infections in different organs such as the blood, heart, bones, and kidneys.

As a MRSA skin infection runs the significant risk of further dissemination, the effect of nanotoxoid(Hla) vaccination on MRSA invasiveness after subcutaneous challenge was studied. Mice were vaccinated with nanotoxoid(Hla), nanotoxoid(−), or PBS on day 0 with a booster dose on day 14 and subcutaneously inoculated with MRSA on day 35. On day 6 post-infection, the bacterial counts in the heart, kidneys, spleen, lungs, and liver were analyzed (Figure 5). In most of the organs that were analyzed, the nanotoxoid(Hla) group showed a significant drop in bacterial burden compared to the nanotoxoid(−) and PBS control groups. Of note, the kidneys and spleen, two organs that traditionally experience heavy bacterial burden per unit weight,[37] both had reductions of approximately two orders of magnitude. The sharp decrease in organ penetration can likely be attributed primarily to better immune management at the site of infection, which results in improved integrity of the skin protective barrier and fewer bacteria entering the circulation system. Additionally, the presence of high amounts of neutralizing titers within the body can further hamper the capacity of invading MRSA bacteria to colonize individual organs, as shown by previous studies on the effect of anti-Hla vaccination in animal models of sepsis.[38] Overall, the results demonstrate that nanotoxoid(Hla) not only prevents superficial damage, but also decreases MRSA invasiveness, which can ultimately help to prevent many of the harsh complications associated with MRSA infections.

3. Conclusion

This study investigated the use of nanoparticle-detained toxins for anti-virulence vaccination as a prophylactic strategy against live MRSA skin infection. Such strategies address an important need in the clinical management of bacterial infections as the rise of antibiotic resistance has been difficult to overcome. An increasing emphasis has been placed on novel strategies that transcend traditional treatment paradigms. The nanotoxoid(Hla) has been shown capable of safely delivering the Hla toxin in its native form without the need for subunit engineering or denaturation. Additionally, the anti-Hla titers elicited by the nanoformulation are of high avidity and long-lived. In the present study, we demonstrated that nanotoxoid(Hla) was capable of promoting strong humoral immunity in an adjuvant-free setting via efficient germinal center formation. Using a mouse skin infection model, it was demonstrated that immunity could substantially attenuate the ability of live bacteria to colonize and systemically invade their hosts, which could ultimately abrogate the negative consequences of severe MRSA infections.

Successful validation of nanotoxoid(Hla) vaccination for protection against live MRSA challenge opens the door for further development of similar platforms against many other common yet deadly bacterial pathogens. Pore-forming toxins are one of the most common protein toxins found in nature, and represent a large class of virulence factors that have natural affinity for cell membrane substrates,[39] and the reported detainment strategy has been shown effective in neutralizing such toxins secreted by several different organisms, including *Staphylococcus aureus, Escherichia coli, and Helicobacter pylori*.[26] By targeting the common mechanism by which many virulence factors function, the nanotoxoid formulation can be applied to an entire class of toxins without specific knowledge of each toxin's precise molecular structure. This strategy opens the door for the nanotoxoid to be used as a diverse vaccine carrier for multi-toxin vaccination, as many pathogens secrete

multiple membrane-attacking virulence factors.[40] By presenting multiple virulent antigens, nanotoxoid can further increase vaccine efficacy and limit bacterial colonization. In addition, changing the membrane coating material[41–43] could further broaden applicability to toxins that do not specifically target RBCs. Overall, the nanoparticle-based anti-virulence vaccine platform is primed to help usher in a new generation of treatments that can address some of the most critical needs in the current management of bacterial infection.

4. Experimental Section

Preparation and characterization of nanotoxoid(Hla)

Red blood cell (RBC) membrane-coated nanoparticles were prepared as previously described.[26] Polymeric cores were made using 0.67 dL/g carboxy-terminated 50:50 poly(lactic-*co*-glycolic acid) (PLGA; LACTEL Absorbable Polymers) with a modified nanoprecipitation method. The polymer was dissolved in acetone at a concentration of 10 mg mL^{-1} and added rapidly to 2 mL of deionized water. The mixture was placed under vacuum for 3 h to evaporate the organic solvent. To obtain the membrane material, RBCs collected from 6-week old male CD-1 mice (Harlan Laboratories) were treated with hypotonic medium and washed multiple times by centrifugation. The final RBC membrane-coated nanoparticles, denoted nanotoxoid(−) were synthesized by sonicating a mixture of the PLGA cores and RBC membrane using a Fisher Scientific FS30D bath sonicator at a frequency of 42 kHz and a power of 100 W for 2 min. The membrane material from 1 mL of mouse blood was used to coat 5 mg of 100 nm PLGA cores. The nanotoxoid(Hla) was generated by incubating 0.2 mg of nanotoxoid(−) with 3 μg of Hla at 37 °C for 15 min. Nanoparticle concentrations for both the nanotoxoid(Hla) and nanotoxoid(−) formulations are expressed as milligrams of PLGA per 1 mL of solution (mg mL^{-1}). The mixture was then filtered through a Sepharose CL-4B (Sigma Aldrich) column to obtain purified nanotoxoid(Hla) free of unbound toxin. The size and the zeta potential of the different nanoformulations were measured by dynamic light scattering (DLS) using a Malvern ZEN 3600 Zetasizer. The structure of the nanotoxoid(Hla) was examined using a Zeiss Libra 120 PLUS EF-TEM Transmission Electron Microscope. Samples were negatively stained with 0.1 wt% uranyl acetate prior to visualization.

Nanotoxoid(Hla) loading analysis

An immunogold staining assay was carried out to confirm insertion of Hla onto the RBC membrane-coated nanoparticles. One drop of nanotoxoid(Hla) or nanotoxoid(−) solution was added onto a glow-discharged carbon coated 400-mesh copper grid (Electron Microscopy Sciences). The grids were then washed before subjecting to blocking with 1 wt % bovine serum albumin (BSA), primary immunostaining with polyclonal rabbit anti-Hla antibody (Sigma Aldrich), and secondary staining with gold-labeled anti-rabbit IgG antibody (Sigma Aldrich). Images were obtained using a Zeiss Libra 120 PLUS EF-TEM Transmission Electron Microscope without negative staining. To analyze Hla retention by dot blot analysis, 1 μL of nanotoxoid(Hla) solution at 2 mg mL^{-1} was dropped onto a nitrocellulose membrane and allowed to fully dry under vacuum. Afterwards, the membrane was blocked with 1 wt% BSA solution and then probed with a polyclonal rabbit anti-Hla primary antibody (Sigma Aldrich) followed by a donkey anti-rabbit IgG-horseradish

peroxidase (HRP) conjugate secondary antibody (Biolegend). The blot was developed with ECL western blotting substrate (Pierce) using a Mini-Medical/90 Developer (ImageWorks). Nanotoxoid(−) solution at 2 mg mL^{-1} was used as negative control and Hla solution corresponding to 100% loading (30 μg mL^{-1}) was used as positive control. Blot intensity was measured by analyzing the mean gray values of dots via Image J software.

Germinal center analysis

All animal experiments followed protocols that were reviewed, approved and performed under the regulatory supervision of the University of California, San Diego's institutional biosafety program and the Institutional Animal Care and Use Committee (IACUC). Six-week old male CD-1 mice (Harlan Laboratories) were immunized subcutaneously in the lateral tarsal region just above the ankle with 0.1 mg of nanotoxoid(Hla). Nanotoxoid(−) and PBS were used as negative controls. On day 21 post-immunization, the mice were euthanized and the draining popliteal lymph nodes were collected for analysis. For immunohistochemical analysis, the lymph nodes were cryosectioned and stained with anti-mouse/human B220-Pacific Blue, anti-mouse IgD-Alexa Fluor 488, and anti-mouse/human GL-7-Alexa Fluor 647 antibodies (Biolegend). For flow cytometry analysis, Lymph nodes were digested in 1 mg mL^{-1} collagenase D (Roche) solution, and stained with the above antibodies. Data was collected using a BD FACSCanto-II flow cytometer and analyzed using Flowjo software.

Anti-Hla titer analysis

Mice were subcutaneously administered with 0.1 mg of nanotoxoid(Hla), 0.1 mg of nanotoxoid(−) or PBS, followed by a boost 14 days later (n=6). On days 0, 14 and 35, the serum of each mouse was collected to assay for Hla-specific antibody titers by an enzyme-linked immunosorbent assay (ELISA). A 96-well plate was coated overnight with 2 μg ml^{-1} Hla using commercial coating buffer (Biolegend). The wells were then blocked with 5 wt% milk before adding serially diluted serum samples as the primary antibody. Goat anti-mouse IgG-HRP (Biolegend) was then employed as the secondary antibody. The plate was developed with 1-Step Slow TMB-ELISA substrate (Pierce) and measured at 450 nm with a Tecan Infinite M200 Multiplate Reader.

MRSA infection and vaccine efficacy

The MRSA strain USA300 TCH1516 (American Type Culture Collection) was used in this study. The bacteria were cultured at 37 °C in tryptic soy broth, harvested by centrifugation, washed, suspended with PBS and adjusted to the appropriate concentration by optical density measurements before use. Mice immunized with 0.1 mg of nanotoxoid(Hla), 0.1 mg of nanotoxoid(−), or PBS on days 0 and 14 were challenged with 1×10^9 CFU of the bacteria on day 35. The bacteria were inoculated subcutaneously in the back region in an area that was carefully shaved using hair clippers before the challenge. The dermonecrotic area was monitored daily and reported as the width multiplied by the height of the visible lesion. On day 6 post-challenge the mice were euthanized, perfused with PBS via the heart, and the skin, heart, liver, spleen, lungs, and kidneys of each mouse were excised and processed for enumeration. Briefly, organs were homogenized in sterile PBS using a Biospec

Mini BeadBeater, diluted 10-fold serially with PBS, plated onto tryptic soy agar, and finally the colonies were counted after 24 h of incubation at 37 °C.

Acknowledgments

This work is supported by the National Institutes of Health under Award Numbers R01EY025947 and R01DK095168 and the National Science Foundation Grant DMR-1505699. R. F. is supported by a National Institutes of Health R25CA153915 training grant from the National Cancer Institute. B. L. is supported by a National Institutes of Health 5F31CA186392 training grant from the National Cancer Institute.

References

1. Howard DH, Scott RD 2nd, Packard R, Jones D. Clin Infect Dis. 2003; 36:S4. [PubMed: 12516025]
2. Bush K, Courvalin P, Dantas G, Davies J, Eisenstein B, Huovinen P, Jacoby GA, Kishony R, Kreiswirth BN, Kutter E, Lerner SA, Levy S, Lewis K, Lomovskaya O, Miller JH, Mobashery S, Piddock LJ, Projan S, Thomas CM, Tomasz A, Tulkens PM, Walsh TR, Watson JD, Witkowski J, Witte W, Wright G, Yeh P, Zgurskaya HI. Nat Rev Microbiol. 2011; 9:894. [PubMed: 22048738]
3. Clatworthy AE, Pierson E, Hung DT. Nat Chem Biol. 2007; 3:541. [PubMed: 17710100]
4. Ramachandran G. Virulence. 2014; 5:213. [PubMed: 24193365]
5. Rasko DA, Sperandio V. Nat Rev Drug Discov. 2010; 9:117. [PubMed: 20081869]
6. Blencowe H, Lawn J, Vandelaer J, Roper M, Cousens S. Int J Epidemiol. 2010; 39:102.
7. Kurosky S, Davis KL, Karve SJ. Value Health. 2014; 17:A278.
8. Cryz SJ Jr, Furer E, Germanier R. Infect Immun. 1982; 38:21. [PubMed: 7141690]
9. Kernodle DS. J Infect Dis. 2011; 203:1692. [PubMed: 21593000]
10. Karauzum H, Adhikari RP, Sarwar J, Devi VS, Abaandou L, Haudenschild C, Mahmoudieh M, Boroun AR, Vu H, Nguyen T, Warfield KL, Shulenin S, Aman MJ. PLoS One. 2013; 8:e65384. [PubMed: 23762356]
11. Klevens RM, Morrison MA, Nadle J, Petit S, Gershman K, Ray S, Harrison LH, Lynfield R, Dumyati G, Townes JM, Craig AS, Zell ER, Fosheim GE, McDougal LK, Carey RB, Fridkin SK. M. I. Active Bacterial Core surveillance. JAMA. 2007; 298:1763. [PubMed: 17940231]
12. Lowy FD. N Engl J Med. 1998; 339:520. [PubMed: 9709046]
13. Rivera AM, Boucher HW. Mayo Clin Proc. 2011; 86:1230. [PubMed: 22134942]
14. Boucher H, Miller LG, Razonable RR. Clin Infect Dis. 2010; 51:S183. [PubMed: 20731576]
15. Otto M. Annu Rev Microbiol. 2010; 64:143. [PubMed: 20825344]
16. Li M, Diep BA, Villaruz AE, Braughton KR, Jiang XF, Deleo FR, Chambers HF, Lu Y, Otto M. Proc Natl Acad Sci USA. 2009; 106:5883. [PubMed: 19293374]
17. Wardenburg JB, Schneewind O. J Exp Med. 2008; 205:287. [PubMed: 18268041]
18. O'Reilly M, de Azavedo JC, Kennedy S, Foster TJ. Microb Pathog. 1986; 1:125. [PubMed: 3508485]
19. Kennedy AD, Wardenburg JB, Gardner DJ, Long D, Whitney AR, Braughton KR, Schneewind O, DeLeo FR. J Infect Dis. 2010; 202:1050. [PubMed: 20726702]
20. Moon JJ, Huang B, Irvine DJ. Adv Mater. 2012; 24:3724. [PubMed: 22641380]
21. Fang RH, Kroll AV, Zhang L. Small. 2015; 11:5483. [PubMed: 26331993]
22. Tao Y, Ju EG, Li ZH, Ren JS, Qu XG. Adv Funct Mater. 2014; 24:1004.
23. Balmert SC, Little SR. Adv Mater. 2012; 24:3757. [PubMed: 22528985]
24. Li Z, Dong K, Zhang Y, Ju E, Chen Z, Ren J, Qu X. Chem Commun. 2015; 51:15975.
25. Li Z, Liu Z, Yin M, Yang X, Renm J, Qu X. Adv Healthc Mater. 2013; 2:1309. [PubMed: 23526798]
26. Hu CM, Fang RH, Copp J, Luk BT, Zhang L. Nat Nanotechnol. 2013; 8:336. [PubMed: 23584215]
27. Wang F, Gao W, Thamphiwatana S, Luk BT, Angsantikul P, Zhang Q, Hu CM, Fang RH, Copp JA, Pornpattananangkul D, Lu W, Zhang L. Adv Mater. 2015; 27:3437. [PubMed: 25931231]
28. Hu CM, Fang RH, Luk BT, Zhang L. Nat Nanotechnol. 2013; 8:933. [PubMed: 24292514]

29. Copp JA, Fang RH, Luk BT, Hu CMJ, Gao WW, Zhang K, Zhang LF. Proc Natl Acad Sci USA. 2014; 111:13481. [PubMed: 25197051]
30. Moon JJ, Suh H, Polhemus ME, Ockenhouse CF, Yadava A, Irvine DJ. PLoS One. 2012; 7:e31472. [PubMed: 22328935]
31. McHeyzer-Williams LJ, McHeyzer-Williams MG. Annu Rev Immunol. 2005; 23:487. [PubMed: 15771579]
32. Moon JJ, Suh H, Li AV, Ockenhouse CF, Yadava A, Irvine DJ. Proc Natl Acad Sci USA. 2012; 109:1080. [PubMed: 22247289]
33. Rao L, Bu LL, Xu JH, Cai B, Yu GT, Yu X, He Z, Huang Q, Li A, Guo SS, Zhang WF, Liu W, Sun ZJ, Wang H, Wang TH, Zhao XZ. Small.
34. DeFranco AL, Rookhuizen DC, Hou B. Immunol Rev. 2012; 247:64. [PubMed: 22500832]
35. Berube BJ, Bubeck Wardenburg J. Toxins (Basel). 2013; 5:1140. [PubMed: 23888516]
36. Miller LS, Cho JS. Nat Rev Immunol. 2011; 11:505. [PubMed: 21720387]
37. Kokai-Kun JF, Chanturiya T, Mond JJ. J Antimicrob Chemother. 2007; 60:1051. [PubMed: 17848374]
38. Adhikari RP, Karauzum H, Sarwar J, Abaandou L, Mahmoudieh M, Boroun AR, Vu H, Nguyen T, Devi VS, Shulenin S, Warfield KL, Aman MJ. PLoS One. 2012; 7:e38567. [PubMed: 22701668]
39. Fang RH, Luk BT, Hu CM, Zhang L. Adv Drug Deliv Rev. 2015; 90:69. [PubMed: 25868452]
40. Aman MJ, Adhikari RP. Toxins (Basel). 2014; 6:950. [PubMed: 24599233]
41. Fang RH, Hu CM, Luk BT, Gao W, Copp JA, Tai Y, O'Connor DE, Zhang L. Nano Lett. 2014; 14:2181. [PubMed: 24673373]
42. Hu CM, Fang RH, Wang KC, Luk BT, Thamphiwatana S, Dehaini D, Nguyen P, Angsantikul P, Wen CH, Kroll AV, Carpenter C, Ramesh M, Qu V, Patel SH, Zhu J, Shi W, Hofman FM, Chen TC, Gao W, Zhang K, Chien S, Zhang L. Nature. 2015; 526:118. [PubMed: 26374997]
43. Gao W, Fang RH, Thamphiwatana S, Luk BT, Li J, Angsantikul P, Zhang Q, Hu CM, Zhang L. Nano Lett. 2015; 15:1403. [PubMed: 25615236]

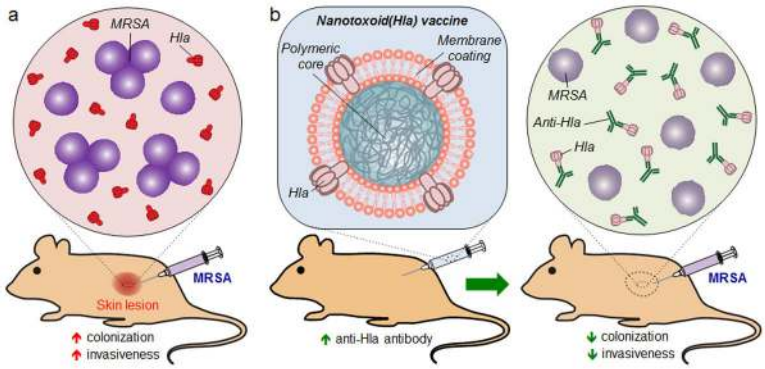

Figure 1. Schematic of nanotoxoid(Hla) protection against MRSA infection

(a) Under normal conditions, MRSA bacteria employ Hla to help them colonize the site of challenge, resulting in significant skin lesion formation and systemic invasiveness. (b) After vaccination with the nanotoxoid(Hla) formulation, anti-Hla titers are induced. These antibodies neutralize the toxin produced by the MRSA bacteria at the site of challenge, reducing the ability of the pathogen to colonize and enter into systemic circulation.

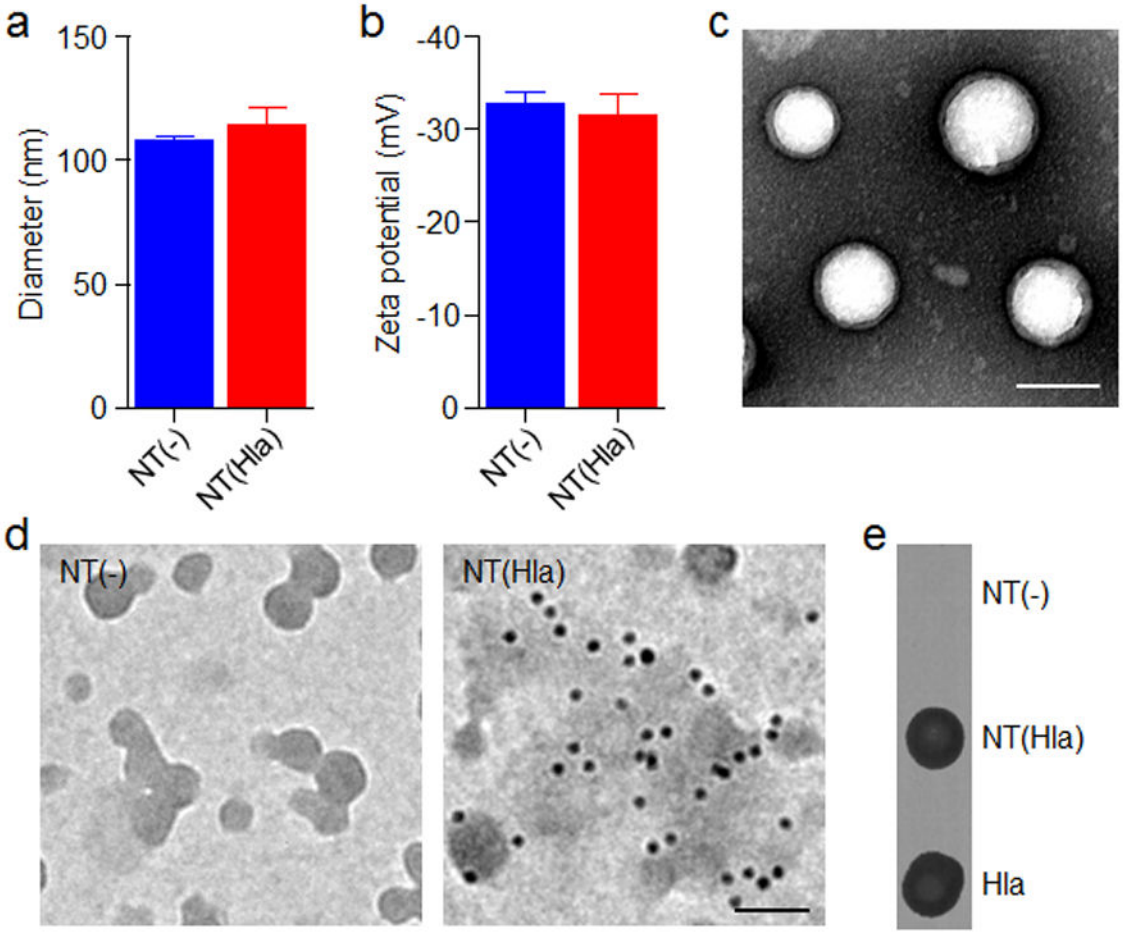

Figure 2. Nanotoxoid(Hla) characterization

(a) Size and (b) zeta potential of nanotoxoid(−) [denoted "NT(−)"] and nanotoxoid(Hla) [denoted "NT(Hla)"] (n=3). Error bars represent standard deviation. (c) TEM image of nanotoxoid(Hla) after negative staining with uranyl acetate. Scale bar = 100 nm. (d) TEM images of immunogold-stained NT(−) and NT(Hla) with anti-Hla as the primary immunostain and gold-labeled anti-IgG as the secondary stain. The gold (~10 nm) appears as dark punctates on the images. Scale bar = 100 nm. (e) Dot blotting results using anti-Hla as the primary immunostain. Quantification by image analysis revealed that 95.2% of the Hla input was retained on the final NT(Hla) formulation.

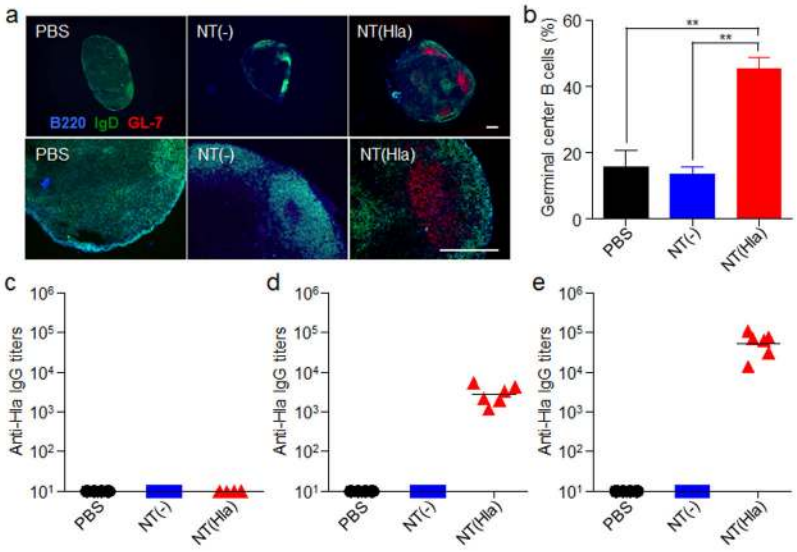

Figure 3. Germinal center formation and antibody production induced by nanotoxoid(Hla) vaccination

(a,b) Mice were vaccinated with PBS, nanotoxoid(−) [NT(−)], or nanotoxoid(Hla) [NT(Hla)] (n=3). The draining lymph nodes were collected 21 days later for the analysis of B220 (blue), IgD (green), and GL-7 (red) expression by either immunohistochemistry (a) or flow cytometry (b). Scale bars = 250 μm. For flow cytometric analysis, cells were first gated on $B220^{+}IgD^{low}$ and the numbers reported are the percentage $GL\text{-}7^{+}$ cells within that population. Error bars represent standard error. Statistical significance determined by one-way ANOVA (** $P < 0.01$). (c–e) Mice were vaccinated with PBS, NT(−), or NT(Hla) on day 0 with a boost on day 14 (n=6). On days 0 (c), 14 (d), and 35 (e), serum was collected and the anti-Hla IgG titers were quantified by ELISA. Lines represent geometric means.

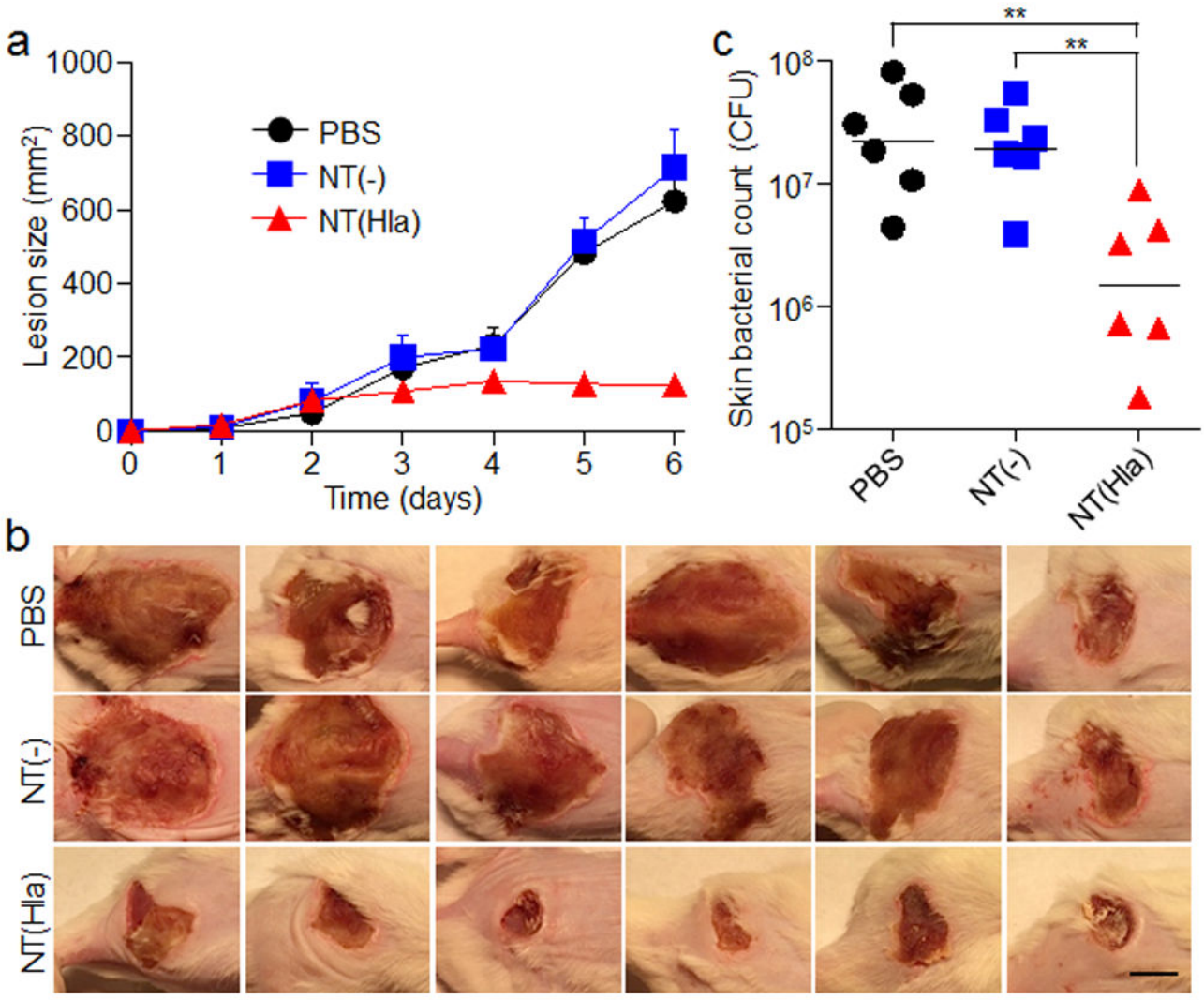

Figure 4. Effect of nanotoxoid (Hla) vaccination on MRSA skin colonization

Mice vaccinated with PBS, nanotoxoid(−) [NT(−)], or nanotoxoid(Hla) [NT(Hla)] on days 0 and 14 were challenged subcutaneously with 1 x 10^9 CFU of MRSA bacteria on day 35. (a) The skin lesions were monitored over the course of 6 days (n=6). Lesion size is reported as the product of the largest and smallest dimensions. Error bars represent standard error. (b) Images of skin lesions on day 6 post-infection. Scale bar = 1 cm. (c) On day 6 post-infection, the affected skin and underlying tissue were collected and the bacterial burden enumerated (n=6). Lines represent geometric mean. Statistical significance determined by one-way ANOVA (**$P < 0.01$).

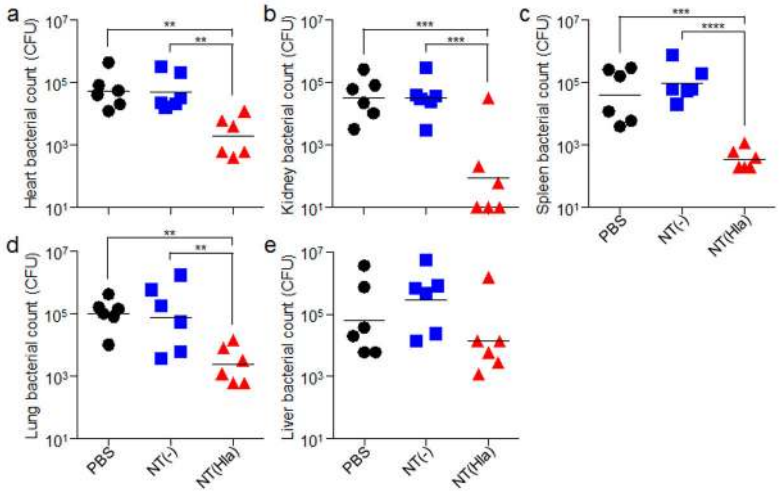

Figure 5. Effect of nanotoxoid(Hla) vaccination on MRSA invasiveness

Mice vaccinated with PBS, nanotoxoid(−) [NT(−)], or nanotoxoid(Hla) [NT(Hla)] on days 0 and 14 were challenged subcutaneously with 1 x 10^9 CFU of MRSA bacteria on day 35. On day 6 post-infection, the major organs, including the heart (a), kidneys (b), spleen (c), lungs (d), and liver (e) were collected and the bacterial burden of each was enumerated (n=6). Lines represent geometric means. Statistical significance determined by one-way ANOVA (**$P < 0.01$, ***$P < 0.001$ and ****$P < 0.0001$).